Microchimica Acta (2019) 186:726
https://doi.org/10.1007/s00604-019-3813-y

ORIGINAL PAPER

Reusable chemiluminescent fiber optic aptasensor for the determination of 17β-estradiol in water samples

Rong Yang[1] · Jiayao Liu[1] · Dan Song[1] · Anna Zhu[2,3] · Wenjuan Xu[1] · Hongliang Wang[1] · Feng Long[1]

Received: 19 April 2019 / Accepted: 10 September 2019

Abstract

A reusable fiber optic chemiluminescent aptasensor (FOCA) is reported for the rapid and sensitive on-site detection of 17β-estradiol (E2), an endocrine-disrupting compound frequently found in water samples. The E2-ovalbumin conjugate (E2-OVA) was covalently immobilized onto the optical fiber as a biorecognition element as well as a transducer. The affinity constant of the E2/aptamer complex was determined to be 1.35×10^6 M^{-1} using the FOCA. An indirect competitive assay was then developed for E2 detection. A certain concentration of HRP-E2 aptamers pre-reacted with samples containing E2 in various concentrations. Part of HRP-E2 aptamers specially bound to the sensor surface after introduction of the mixture. This catalyzed the chemiluminescece reaction of a chemiluminescent system composed of luminol and H_2O_2. A higher concentration of E2 led to less HRP-E2 aptamer bound to the biosensor surface, thus resulting in less chemiluminescence. Highly sensitive detection of E2 was achieved under optimal conditions, and the limit of detection is 48 ng $\cdot L^{-1}$ (0.18 nM). The whole analytical process, including measurement and regeneration, can be performed in <15 min. The robustness of the biosensor allows its application to multiple assays with little activity loss. The selectivity, recovery, and accuracy of the sensor was demonstrated by evaluating its response to potentially interfering endocrine disruptors in spiked water samples.

Keywords Endocrine disrupting compounds · Aptamer · Chemiluminescence · Fiber optic · Affinity constant

Introduction

Endocrine disrupting compounds (EDCs) comprise a large group of contaminants that can antagonize or mimic the effects of endogenous hormones and are subject to routine monitoring in bodies of water, according to the United States Environmental Protection Agency's (USEPA's) Unregulated Contaminant Monitoring Regulation (UCMR3) [1, 2]. Among EDCs, 17β-estradiol (E2), one of the most important environmental endogenous estrogens, may result in immunological and reproductive system diseases, birth defects, and cancer [3–6]. E2 has been detected in various water bodies at ng·L^{-1} to mg·L^{-1} levels [2, 7]. Even trace levels of E2 can interfere with the normal endocrine functions of humans and other animals through food chain accumulation. To ensure human safety and protect the environment, stringent limits for E2 in bodies of water have been proposed by various regulatory agencies [2, 7]. The USEPA proposed a maximum residue of 1.47 pM for E2 in surface water, and Japan enforced new regulations to limit E2 to 0.294 nM in drinking water [3, 8]. The Codex Alimentarius Commission (CAC) stipulated that estradiol levels should be such that they could not be detected in animal food. Conventional technologies, such as high-performance liquid chromatography (HPLC), gas chromatography–mass spectrometry (GC-MS), and HPLC/MS, have been extensively employed to detect E2 with high accuracy and sensitivity [8–10]. However, these technologies are not suitable for rapid, real-time, and high-frequency analysis as they require expensive instrumentation, a time-consuming analysis process, a large volume of harmful solvents, and professional operation [2, 11]. Hence, it is essential to develop a convenient and rapid analytical technology to detect E2 with high sensitivity and selectivity to protect public health.

Electronic supplementary material The online version of this article (https://doi.org/10.1007/s00604-019-3813-y) contains supplementary material, which is available to authorized users.

✉ Feng Long
longf04@ruc.edu.cn

[1] School of Environment and Natural Resources, Renmin University of China, Beijing 100872, China

[2] Research Institute of Chemical Defense, Beijing 102205, China

[3] State Key Laboratory of NBC Protection for Civilian, Beijing 102205, China

Published online: 27 October 2019

Considerable interest exists in developing biosensors to detect trace E2 in water samples because of their rapidity, sensitivity, and specificity. Antibodies are the most commonly used biorecognition molecules for biosensor construction [12, 13]. However, antibody production is time consuming and antibodies are susceptible to external environmental conditions [3]. Aptamers—single strands of DNA or RNA—have appeared as a useful alternative as biosensing molecules, owing to their unique characterizations [3, 14]. Aptamers selected in vitro can be economically produced via chemical synthesis, are more stable than antibodies, and are more resistant to denaturation and degradation [3, 14]. An aptamer can fold into tertiary structures to form binding pockets for its target and specifically bind with it through hydrogen bonds, electrostatic interactions, and hydrophobic interactions [15]. Although various technologies (e.g., surface plasmon resonance and microscale thermophoresis) have been used to determine aptamer–small molecule interactions, these technologies are complex and expensive for analysis to maintain high sensitivity [16, 17]. Since the E2 aptamer was first reported by Kim et al. [18], various E2 aptasensors (e.g., colorimetric, electrochemical, and fluorescence) have been reported for E2 detection [2, 3, 14]. A nanomaterials-based colorimetric aptasensor is cost effective and simple, but it is susceptible to sample matrixes and low sensitivity [19]. Electrochemical aptasensors have high sensitivity and selectivity, but their stability and reproducibility pose a major obstacle for practical applications [20]. A "turn-on" fluorescence aptasensor was developed for sensitive detection of E2 [11]. However, challenges still remain in improving aptasensor robustness, reusability, reproducibility, and ease of use, as well as in how to simplify the complicated design and assay process for rapid on-site detection of E2 and its interaction with the aptamer.

Chemiluminescent (CL) biosensors are suitable for rapid on-site detection of trace targets because of their unique advantages, such as their high sensitivity, wide linear range, low background noise, and no need for an excitation light source [21–23]. Our group developed a compact, inexpensive, easy-to-use, and portable fiber-optic CL platform for the immunoassay of microcystin-LR [24]. By integrating the advantages of this fiber-optic CL platform and the aptamer, a reusable fiber-optic CL aptasensor (FOCA) was built for the first time to use in rapid, highly specific, and sensitive detection of E2 based on the indirect competitive bioassay principle. In this system, a multimode fiber optic was modified by E2-ovalbumin (E2-OVA) conjugates to be used as a biorecognition element and a CL transducer. HRP-E2 aptamers were applied to the reporter molecules for the rapid and sensitive detection of E2. The stability and reusability of the sensing surface and the interference of compounds structurally similar to E2 were evaluated. The feasibility of the FOCA system for detecting real water samples was verified.

Materials and methods

Chemicals and materials

The hapten-protein conjugate E2-OVA was purchased from Beijing Kwinbon Biotechnology Co., Ltd. (www.kwinbon.com). 3-Mercaptopropyl-trimethoxysilane (MTS), N-(4-maleimidobutyryloxy) succinimide (GMBS), sodium dodecyl sulfate (SDS), bovine serum albumin (BSA), ethylene diamine tetraacetic acid (EDTA), and E2 were purchased from Sigma-Aldrich (https://www.sigmaaldrich.com/china-mainland). The CL substrate, a HRP-H_2O_2-luminol system, was bought from Beijing Yisen Biotechnology Co., Ltd. (www.bioyisen.com). Methanol, ethanol, H_2SO_4, H_2O_2, and other reagents, unless specified, were all purchased from Sinapharm Chemical Reagent Beijing Co., Ltd. (www.crc-bj.com).

The HRP-E2 aptamer, 5′-(HRP)-GCT-TCC-AGC-TTA-TTG-AAT-TAC-ACG-CAG-AGG-GTA-GCG-GCT-CTG-CGC-ATT-CAA-TTG-CTG-CGC-GCT-GAA-GCG-CGG-AAG-C-3′, and the HRP-labeled, nonspecific DNA sequence (HRP-n-DNA), 5′-(HRP)-GAT-CGG-GTG-TGG-GTG-GCG-TAA-AGG-GAG-CAT-CGG-ACA-3′, were purchased from Takara Biomedical Technology Co., Ltd. (www.takara.com.cn). The aptamer was dissolved by TE buffer (10 mM Tris-HCl and 10 mM EDTA; pH 8.0); E2 standard solutions were prepared from a stock solution by serial dilutions with 10 mM Tris-HCl buffer. An SDS solution (0.5%; pH = 1.9) was applied for the regeneration of the biosensing surface.

Construction of the fiber-optic chemiluminescent (CL) aptasensor system

A schematic of the constructed FOCA used for CL detection of E2 is shown in Fig. 1. This elegantly simplified FOCA system uses an innovative optical structure consisting of a fiber-optic biosensor and a Si-based photodiode detector to detect CL signals. The fiber-optic biosensor modified by E2-OVA was regarded as a biorecognition element, which was embedded in a black cylindrical sample cell (ϕ = 1.5 mm, length = 35 mm length, and effective volume ~ 60 μL) to block environmental light. The CL signal was collected by the same fiber-optic biosensor. Instead of a PMT, an Si-based photodiode detector (PD-3000) was directly placed at the end of the fiber-optic biosensor to detect the CL intensity. Because the FOCA had no other separated optical elements, the detection efficiency of the CL intensity greatly improved. To achieve an automated measurement, a flow sampling

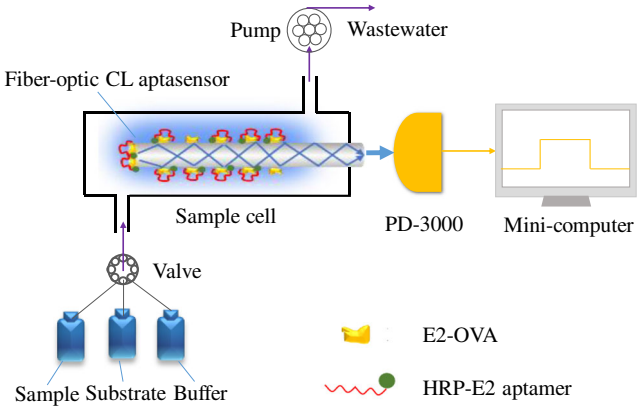

Fig. 1 Schematic diagram of the FOCA system. The FOCA consisted of fiber optic CL aptasensor, valve, pump, photodiode detector, and mini-computer. The elegantly simplified FOCA system utilizes the innovative incorporation of a fiber-optic biosensor and an Si-based photodiode detector, which results in a powerful method to quantify the analyte

system including a peristaltic pump, a six-way injection valve, and a sample cell was used. Various solutions (e.g., buffer, samples, and regeneration solution) were successively introduced into the sample cell. Data acquisition and analysis were achieved by using measurement software.

Fabrication of the biosensing surface

According to our previous results [25], the fiber-optic biosensor modified by hapten-protein conjugates can retain >100 successive assays with little activity loss. Therefore, the E2 hapten-protein conjugates, E2-OVA, are covalently immobilized on the fiber-optic biosensor surface as biorecognition molecules and a CL transducer. The fabrication of biosensing surface is performed according to the method described previously, with a minor adjustment [24, 25] (see Supporting information).

Kinetic analysis of E2–aptamer interactions

The affinity constant is a key kinetic parameter used to characterize the E2–aptamer interaction as well as to develop the highly sensitive E2 aptasensor [11]. To determine the affinity constant of the E2–aptamer interaction, a mathematical model was derived to fit the kinetic data. When the HRP-E2 aptamer at various concentrations is introduced over the biosensor surface modified by E2-OVA, the binding reaction that occurs on the biosensor surface can be expressed by

$$\mathrm{E} + \mathrm{A} \underset{k_{\mathrm{off}}}{\overset{k_{\mathrm{on}}}{\rightleftharpoons}} \mathrm{E{\cdot}A} \tag{1}$$

where E and A denote E2-OVA modified on the biosensor surface and HRP-E2 aptamer in the solution, respectively. E·A denotes the binding complex of HRP-E2 aptamer with E2 on the biosensor surface. The affinity constant, K_a, for the binding reaction in Eq. (1) can be expressed by

$$K_a = [\mathrm{E} \cdot \mathrm{A}]/[\mathrm{E}][\mathrm{A}]. \tag{2}$$

Given that Langmuir adsorption can be assumed for binding the aptamer to E2 and that the total surface concentration of E2 on the biosensor surface is assumed to be $[E]^T$, the following equation can be derived:

$$[E\ A]/[E]^T = K_a[A]_0/\left(1 + K_a[A]_0\right) \tag{3}$$

where $[A]_0$ is the concentration of the E2 aptamer. In this case, because the change in the CL signal, I_{cL}, is proportional to the surface concentration of HRP-E2 aptamer bound to the biosensor surface, I_{cL} can be rewritten as

$$I_{\mathrm{CL}}/I_{\mathrm{CL,max}} = K_a[\mathrm{A}]_0/\left(1 + K_a[\mathrm{A}]_0\right), \tag{4}$$

where I_{CL} is the CL intensity when a balanced state is obtained at a certain concentration of HRP-E2 aptamer, and $I_{CL,max}$ is the maximum CL intensity when all binding sites of the biosensor surface are occupied by the HRP-E2 aptamer.

The following equation can be derived from Eq. (4):

$$1/I_{\mathrm{CL}} = 1/I_{\mathrm{CL,max}} + 1/\left(K_a[\mathrm{A}]_0 I_{\mathrm{CL,max}}\right). \tag{5}$$

As shown in Eq. (5), a straight line of slope $1/(K_a I_{CL,max})$ and an x intercept of $1/I_{CL,max}$ is obtained when $1/I_{CL}$ is plotted against $1/[A]_0$, and the equilibrium affinity constant K_a can be calculated after testing various concentrations of HRP-E2 aptamer.

Results and discussion

Feasibility of using the E2-OVA–modified biosensor

E2-OVA conjugates were covalently modified on the fiber-optic biosensor surface using GMBS as a bifunctional reagent, and the modified fiber-optic biosensor was regarded as a biorecognition element and CL transducer. To evaluate the feasibility of the E2-OVA–modified biosensor for E2 CL detection, several control experiments were performed as follows (Fig. 2). First, an HRP-n-DNA sequence was introduced into the sample cell for 400 s incubation. After the sample was washed with Tris-HCl buffer, a small CL signal was observed when the CL substrate solution was added. This might contribute to the nonspecific adsorption of part of the HRP-n-DNA on the biosensor surface owing to the electronegativity of DNA. Second, 50.0 nM HRP-E2 aptamer was introduced for 400 s incubation, and the CL substrate solution was introduced after the sample was washed with Tris-HCl buffer. A strong CL signal was detected; the effective CL signal was a factor of 3 higher than that of the HRP-n-DNA sequence. This result demonstrated that the HRP-E2 aptamer bound with E2-

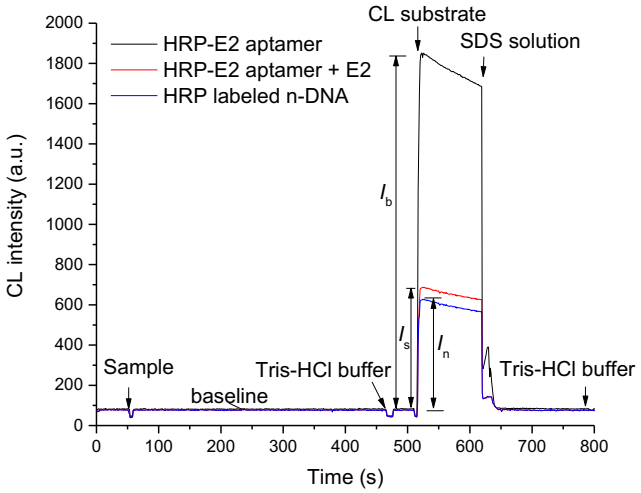

Fig. 2 Assessment of the immobilization effectiveness and specific binding between E2 immobilized onto a fiber-optic biosensor and the HRP-E2 aptamer. The concentrations of HRP-E2 aptamer, HRP-labeled n-DNA, and E2 were 50.0 nM, 50.0 nM, and 1000.0 μg·L^{-1}, respectively. The ionic strength was 350 mM and the pH was 6.0

OVA, because of the specific binding between the E2 aptamer and E2-OVA modified on the biosensor surface, and that the CL reaction occurred under HRP catalysis.

To further verify the above result, a sample mixture of 50.0 nM HRP-E2 aptamer and 1000.0 μg·L^{-1} E2 was introduced into the cell for 400 s incubation; the CL substrate solution was introduced after the sample was washed with Tris-HCl buffer. The CL signal increased, but the increase was similar to that of HRP-n-DNA. This result demonstrated that almost all of the HRP-E2 aptamers were bound to free E2 because of its high concentration, and few HRP-E2 aptamers were bound to the E2-OVA on the biosensor surface; the CL signal should contribute to the nonspecific adsorption of the complex of HRP-E2 aptamer and E2. These results confirmed that the E2-OVA conjugates were successfully modified on the biosensor surface and that the observed CL signal mainly originated from the specific reaction between the HRP-E2 aptamer and the E2-OVA modified on the biosensor surface. Although the HRP-n-DNA or the complex of HRP-E2 aptamer and E2 could nonspecifically adsorb on the biosensor surface, the HRP-E2 aptamer could specifically bind with the E2-OVA immobilized on the biosensor surface and yield the higher CL signal. Furthermore, the addition of E2 into the HRP-E2 aptamer solution resulted in a decrease in the detected CL signal. Therefore, our aptasensor can be applied in E2 detection.

Figure 2 shows exemplary real-time CL signals for one analysis cycle. For each assay, the CL intensity, which was used for obtaining the dose–response relationships later, was calculated as follows:

$$I_b = (\text{CL } \textit{intensity} \text{ at } \textit{the peak value}–\text{CL } \textit{intensity} \text{ at } \textit{the baseline}) \textit{ of the blank}, \quad (6)$$

$$I_s = (\text{CL } \textit{intensity} \text{ at } \textit{the peak value}–\text{CL } \textit{intensity} \text{ at } \textit{the baseline}) \textit{ of the sample}, \quad (7)$$

$$I_n = (\text{CL } \textit{intensity} \text{ at } \textit{the peak value}–\text{CL } \textit{intensity} \text{ at } \textit{the baseline}) \textit{ of } \text{n-DNA}, \quad (8)$$

$$E_s = (I_b–I_s)/(I_b–I_n) \text{ (a.u.CL } \textit{intensity}). \quad (9)$$

Optimization of detection conditions

To achieve highly sensitive detection of E2, it is essential to optimize detection conditions such as the ionic strength, pH value, HRP-E2 aptamer concentration, and reaction time between the HRP-E2 aptamer and the E2-OVA immobilized on the biosensor surface [26, 27]. Initially, the pH value and reaction time between the HRP-E2 aptamer and the E2-OVA was optimized, and the results were shown in Fig. S1 and Fig.S2. The optimal pH and incubation time were determined as 6.0 and 400 s, respectively.

The E2–aptamer affinity interaction greatly depends on the ionic strength of the solution [27]. Figure 3a shows a plot of the CL intensity as a function of various concentrations of NaCl (0–500 mM) in the Tris-HCl buffer. When the concentration of NaCl was <350 mM, the CL intensity of the aptasensor increased with increasing ionic strength for the HRP-E2 aptamer of each concentration. When the NaCl concentration was >350 mM, the CL intensity of the aptasensor decreased. This effect can be connected with the shielding of the negative charges at the aptamer as well as at the protein surface. At low ion concentrations, the existence of cations neutralized the negative charge of the DNA and the protein to reduce their repulsive force [14, 28]. However, an excess number of cations increased the repulsive force because the DNA and protein both carried a positive charge under such circumstances [29]. Thus, the ionic strength had a substantial influence on the E2 aptasensor and should be taken into account in its practical application. The 350 mM NaCl was selected for the following tests.

To optimize the HRP-E2 aptamer concentration, several concentrations of HRP-E2 aptamer were directly introduced into the cell for pre-reaction. After the sample was washed with Tris-HCl buffer, the CL substrates were added and the CL signal was recorded. The mixture of HRP-E2 aptamer at various concentrations and 10.0 μg·L^{-1} E2 was delivered into the cell for testing. As shown in Fig. S3, the CL signal increased with the increase in aptamer concentration because more HRP-E2 aptamers were bound to the E2-OVA conjugates immobilized on the biosensor surface. However, the sensitivity index ($\varepsilon = [I_b - I_s]/I_b$, where I_b and I_s represent the CL intensities without E2 and with 10.0 μg·L^{-1} E2, respectively) deteriorated with increasing aptamer concentration (Fig. 3b). This indicated that a low aptamer concentration was favorable to improve the sensitivity of the aptasensor. By

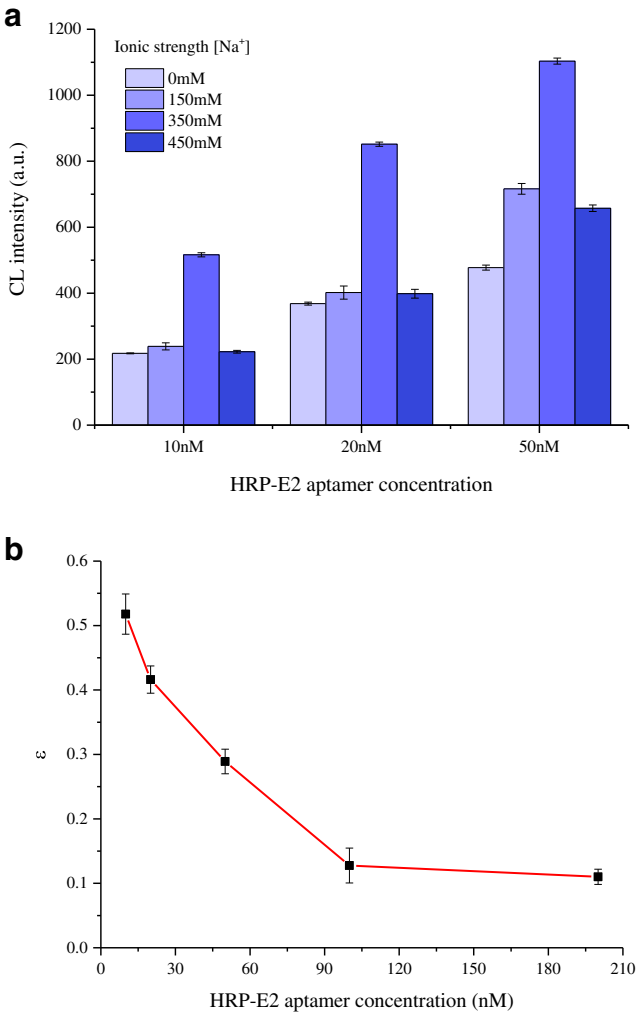

Fig. 3 Optimization of detection conditions for the E2 aptasensor. **a** Effect of ionic strength on the CL intensity of the E2 aptasensor. The HRP-E2 aptamer concentrations were 10.0, 20.0, and 50.0 nM; the concentrations of NaCl were 0, 150.0, 350.0, and 450.0 mM; and the incubation time was 400 s. **b** Effect of HRP-E2 aptamer concentration on the sensitivity index (ε). The HRP-E2 aptamer concentrations were 10.0, 20.0, 50.0, 100.0, and 200.0 nM; the concentration of NaCl was 350.0 mM; and the incubation time was 400 s. The error bars correspond to the standard deviation of the data points in three repeated experiments ($n = 3$)

considering the CL intensity level required, 50.0 nM HRP-E2 aptamer was regarded as the optimal concentration for E2 detection even though a lower concentration of aptamer can provide a higher sensitivity index.

Kinetics analysis of E2–aptamer interactions

Compared with antibodies, aptamers are ideal candidates for biosensors in medical diagnostics and environmental monitoring because they are easier to obtain, more stable, and more resistant to biodegradation [14]. The most common approach to elucidate biomolecular interactions entails affinity-based methods. The affinity constant between an aptamer and its target is a critical factor that affects the sensitivity of aptasensors [29]. Herein, the FOCA was applied to investigate the E2–aptamer affinity constant. To evaluate their affinity constant, HRP-E2 aptamers of various concentrations (from 10.0 to 200.0 nM) were introduced into the sample cell for a 400 s reaction. After the sample was washed with Tris-HCl buffer solution, the CL substrate was added and the CL signal was measured.

The relationship between the aptamer concentration and the CL intensity is shown in Fig. 4a. Plots summarizing the concentration-dependent E2 aptamer binding to E2-OVA conjugates exhibited a characteristic linear response at low concentrations and saturation at higher concentrations. According to Eq. (5), $1/I_{CL}$ was plotted against $1/[A]_0$ as shown in Fig.

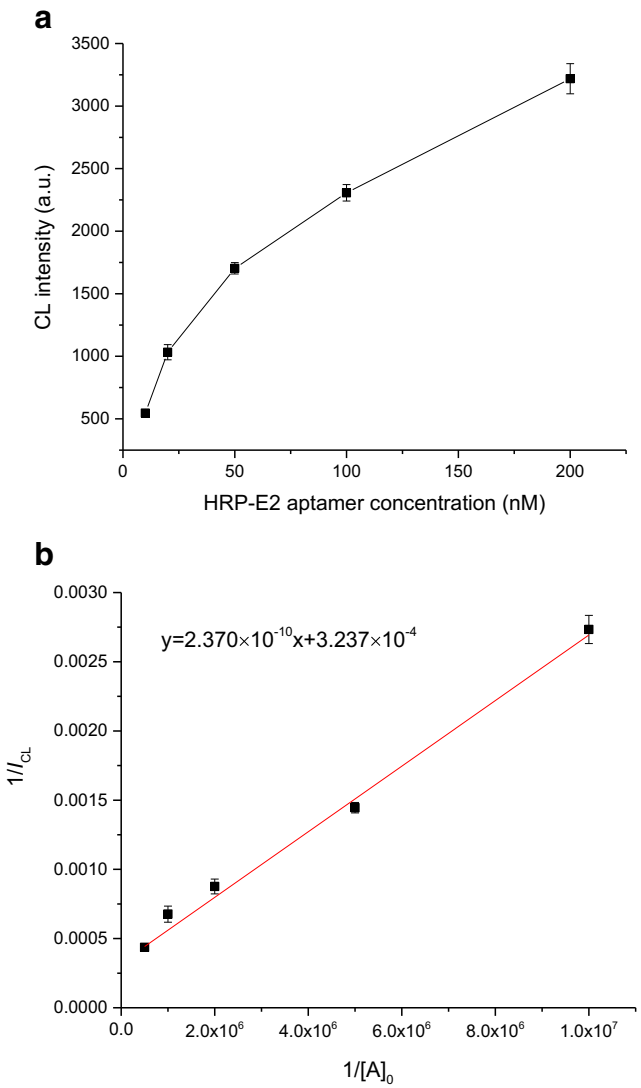

Fig. 4 The FOCA served as a quantitative assay platform for binding kinetics between E2 and its aptamer. **a** CL intensity of the HRP-E2 aptamer at various concentrations (10.0, 20.0, 50.0, 100.0, and 200.0 nM). **b** Dependence of $1/I_{CL}$ on $1/[A]_0$ for the association between the HRP-E2 aptamer and E2. The error bars correspond to the standard deviation of the data points in three repeated experiments ($n = 3$)

4b. Good linear relationships between $1/I_{CL}$ and $1/[A]_0$ were obtained, indicating that first-order kinetics held. The E2–aptamer affinity constant (K_a) was determined as $1.35 \times 10^6\ M^{-1}$ (or $K_D = 0.74\ \mu M$). This affinity constant was slightly lower than those determined by other affinity methods [16, 18], which illustrates that the binding profile of the aptamer is often influenced by the nature of the assay and its application format (e.g., HRP labeled). Our result demonstrated that the FOCA can serve as a simple and quantitative assay platform for the analysis of interactions between aptamers and small molecules based on the proposed theory.

CL bioassay of E2

The indirect competitive bioassay principle was applied for the quantitative detection of E2 under optimal conditions. Figure 5a illustrates the CL detection mechanism of the E2 aptasensor using the FOCA. Initially, 50.0 μL of samples containing E2 at various concentrations and 50.0 μL of 50 nM HRP-E2 aptamer were mixed and pre-reacted for 5 min. During this period, some of the HRP-E2 aptamers specifically bound with E2, in proportion to the concentration of E2 in the samples. Then, the mixture was added to the sample cell. The HRP-E2 aptamers that were not bound with E2 in solution can bind to the E2-OVA–modified biosensor surface. After the samples were rinsed with Tris-HCl buffer to remove any excess HRP-E2 aptamers, 100.0 μL CL substrate solution was introduced into the cell. The HRP-E2 aptamers bound with E2-OVA catalyzed the luminescence of substrates, and the CL intensity was recorded in real time. Finally, the biosensor surface was regenerated using a 0.5% SDS solution (pH = 1.9). After washing with Tris-HCl buffer, the biosensor could be reused for the next test.

Typical time-dependent traces recorded by the FOCA are shown in Fig. 5**b**. The Calibration curve for E2, plotted against the logarithm of the concentration of E2 using a four-parameter logistic equation (see Supporting Information), is shown in Fig. 5**c**. The error bars in Fig. 5c correspond to the standard deviation of the data points ($n = 3$), which was <4.1%, indicating the good stability of the FOCA for E2 detection. The limit of detection (LOD) of E2 was 0.048 $\mu g \cdot L^{-1}$ (0.18 nM) using three times the standard deviation of the mean blank values, and the linear response ranged from 0.32 to 112.2 $\mu g \cdot L^{-1}$ (1.17 ~ 411.9 nM). This LOD meets the regulatory requirements of both the European Union (0.05 $\mu g \cdot L^{-1}$) and the United States Food and Drug Administration (0.12 $\mu g \cdot L^{-1}$).

The high sensitivity of the E2 aptasensor might be caused by the following. First, increasing the amount of E2-OVA on the fiber-optic biosensor surface through modifying both its distal end and cylindrical surface could have decreased the HRP-E2 aptamer concentration to yield the same CL intensity. The lower HRP-E2 aptamer concentration had a higher sensitivity index, as described above. Second, the surface chemistry of the E2-OVA conjugates on the biosensor surface could have kept their high activity toward the HRP-E2 aptamer for multiple assay cycles, which improved the detection sensitivity and accuracy. Third, unlike the sandwich-like immunosensor of small molecules, which generally need a primary antibody and HRP-labeled secondary antibody for immunoassay [24], our aptasensor applied only the HRP-E2 aptamer for E2 detection, which had a better reaction activity. Furthermore, the use of the HRP-E2 aptamer greatly simplified the detection process and shortened the assay time (to <15 min). Compared with other methods (Supporting information), the FOCA system had other advantages, including the simple system structure because of the free magnetic beads and PMT, the small sample volume, and the high reusability and portability.

Reusability and selectivity of the sensor

To ensure the accuracy of the detection results, good regeneration and binding properties of the biosensor surface are critical for the reusability of the aptasensor. The traditional CL immunoassay methods use immune-magnetic beads to capture targets and to detect targets; these beads are not generally reused, thus leading to high detection costs and inaccurate results [2, 11]. The reusability, stability, and activity of the biosensor modified with E2-OVA conjugate was evaluated through numerous bioassays (Fig. S4). The performance of the biosensor was verified using blank samples without E2 every 10 times, and the biosensor could be reused at least 150 times with little activity loss (<6.5%). After each E2 detection cycle, the noncovalently bound aptamer was completely removed, and the active biosensor surface was regenerated with an SDS solution.

The selectivity of aptasensors is another important parameter affecting the specificity and reliability of bioassays. To assess the selectivity of the E2 aptasensor, its responses to potentially interfering materials, such as oestrone (E1), estriol (E3), diethylstilbestrol (DES), nonylphenol (NP), and alkylphenol (OP) (1000.0 $\mu g \cdot L^{-1}$), were evaluated. As shown in Fig. 6, E1, E3, and DES could decrease the CL intensity of the E2 aptasensor at high concentrations; DES had a maximum inhibition for the E2 aptamer, with a CL intensity of ~76% of the blank sample. However, those intensities were far higher than that of E2 (~3% of the blank sample). The addition of NP and OP barely decreased the CL intensity. These results indicate that the aptasensor was highly selective for E2.

Analysis of real water samples and their evaluation by enzyme-linked immunosorbent assay

The evaluation of matrix effects in real samples is essential to assessing the newly developed CL aptasensor because these effects may affect E2–aptamer binding [2, 30]. A recovery

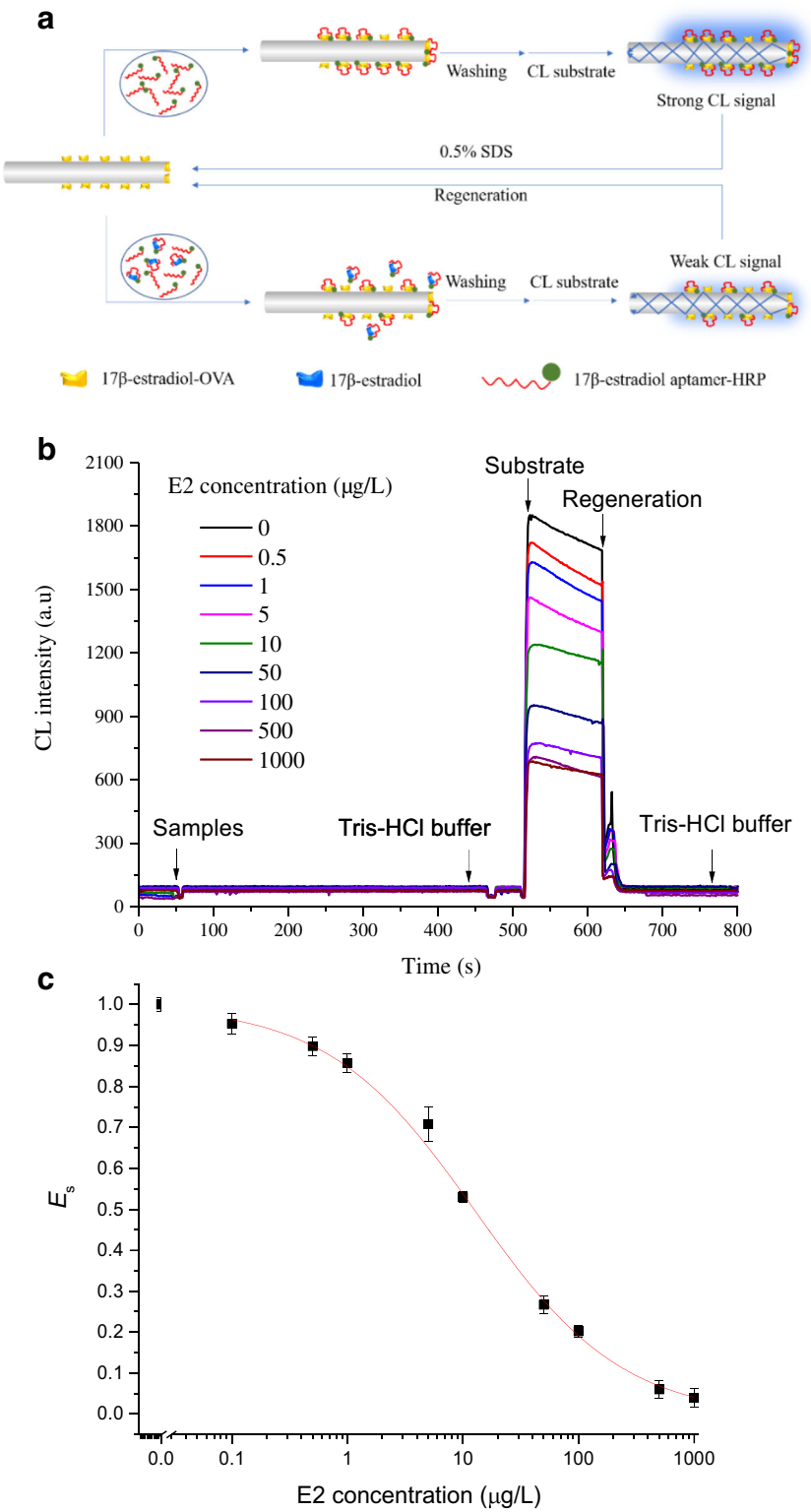

Fig. 5 The FOCA allowed quantification of E2 based on the indirect competitive bioassay principle. **a** Schematic of sensing mechanism of E2 using the FOCA. **b** Typical sensing response curves at different E2 concentrations ranging from 0 to 1000.0 μg·L^{-1} (with 50.0 nM HRP-E2 aptamer). **c** Calibration curve for E2 detection (E2 concentrations ranged from 0 to 1000.0 μg·L^{-1} and 50.0 nM HRP-E2 aptamer). The error bars correspond to the standard deviation of the data points in three repeated experiments ($n = 3$)

study was performed using several real water samples, including laboratory tap water, commercially available bottled water, and effluent of a wastewater treatment plant. These water samples were spiked with E2 from the stock solution at various concentrations (20.0, 40.0, and 60.0 μg·L^{-1}). Then, 50.0 μL of samples containing E2 at various spiked concentrations and 50.0 μL of 50 nM HRP-E2 aptamer were mixed and pre-reacted for 5 min. Then, the mixture was pumped into the sample cell and detected using the FOCA. The results are summarized in Table 1.

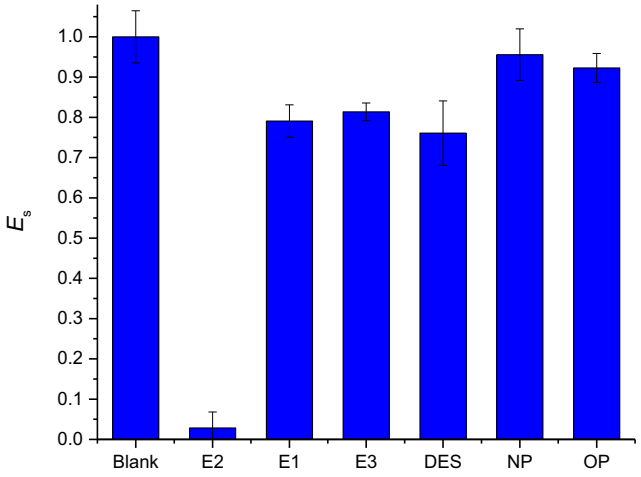

Fig. 6 Comparison of sensing signal of various potentially interfering materials (E1, E3, DES, NP, and OP) at a concentration of 1000.0 μg·L^{-1}. The HRP-E2 aptamer concentration was 50.0 nM. The error bars correspond to the standard deviation of the data points in three repeated experiments ($n = 3$)

Satisfactory recoveries were obtained within the linear concentration range. The average recoveries of the spiked samples varied from 80.3% to 105.7%. Parallel test results showed that the relative standard deviation (RSD) was <9.2%. These results are comparable with those obtained from the analysis of the same spiked samples by enzyme-linked immunosorbent assay (ELISA). All of these results demonstrate that any possible interference from the different background compositions of real water samples on the aptasensor was negligible. The accuracy and reliability of the present method confirmed the application potential of the aptasensor for accurate E2 detection in real water samples.

Conclusions

A simple and reusable CL aptasensor for the sensitive and specific detection of E2 was developed by integrating the advantages of a fiber-optic CL biosensing platform and an aptamer. In this system, the fiber-optic biosensor, modified by E2-OVA conjugates instead of the traditional immune-magnetic beads, was regarded as the biorecognition element as well as the transducer. E2 detection was performed by the FOCA with high sensitivity, accuracy, and rapidity, and the LOD of E2 was 0.048 μg·L^{-1} (0.18 nM) under optimal conditions. Through combining the FOCA with a nanomaterial-based signal amplification system, a highly sensitive chemiluminescent FOCA system can be achieved (ref.). Determination of the E2–aptamer affinity constant was also achieved by using the FOCA based on the proposed theory, and the K_a was 1.35×10^6 M^{-1}.

Compared with CL immunoassay and other biosensors, the CL E2 aptasensor had several advantages. First, the robustness of the E2-OVA–modified biosensor surface allowed multiple E2 detection cycles with little activity loss, which made the biosensor accurate and cost effective. Second, an HRP-labeled aptamer was used as the biocaptured probe, which was easier to produce and cheaper than the HRP-labeled antibody in CL immunoassay. Third, the indirect competitive bioassay mode (instead of a sandwich immunoassay) could simplify the detection operation and shorten the detection time [11]. The whole analysis process, including measurement and regeneration, took less than 15 min. Fourth, the FOCA could also become a powerful tool for mapping the binding affinities of interactions between various aptamers and small molecules. In addition, measurement of E2-spiked water samples using the FOCA showed good recovery, precision, and accuracy, all of which were consistent with the results of ELISA. Therefore, the

Table 1 E2 FOCA and ELISA recovery in spiked water samples ($n = 3$)

Water sample	Spiked (μg·L^{-1})	FOCA			ELISA		
		Measured (μg·L^{-1})	Recovery (%)	RSD (%)	Measured (μg·L^{-1})	Recovery (%)	RSD (%)
Effluent of wastewater treatment plant	20.0	17.16	85.8%	9.2%	16.04	80.2%	7.0%
	40.0	41.16	102.9%	6.8%	37.08	92.7%	5.4%
	60.0	56.24	93.7%	8.3%	46.8	78.0%	2.9%
Bottled water	20.0	21.14	105.7%	3.4%	20.84	104.2%	2.0%
	40.0	36.76	91.9%	1.9%	36.92	92.3%	4.9%
	60.0	62.76	104.6%	8.4%	68.64	114.4%	2.0%
Tap water	20.0	19.12	95.6%	5.3%	16.84	84.2%	0.1%
	40.0	36.04	90.1%	5.8%	37.01	92.5%	1.2%
	60.0	48.18	80.3%	7.2%	45.78	76.3%	1.1%

All samples were collected on the 18 December, 2018, and the initial concentration of E2 in them was undetectable (<0.048 μg·L^{-1})

FOCA system not only provides a simple quantitative platform for interactions between aptamers and small molecules but also can be readily extended toward the rapid and sensitive on-site monitoring of other targets.

Acknowledgments This work was supported by the National Natural Science Foundation of China (21675171 and 21277173), the National Instrument Major Project of China (2012YQ3011105), and special funds for central universities to build world-class universities (disciplines) and their distinctive development (20190001).

Compliance with ethical standards

Conflict of interest The authors declare no conflicts of interest.

References

1. Tiziana S, Cristina P, Renato R, Elisabetta F, Giorgio G (2009) The endocrine disrupting activity of surface waters and of wastewater treatment plant effluents in relation to chlorination. Chemosphere 75:335–340
2. Yildirim N, Long F, Gao C, He M, Shi HC, Gu AZ (2012) Aptamer-based optical biosensor for rapid and sensitive detection of 17β-estradiol in water samples. Environ Sci Technol 46:3288–3294
3. Nezami A, Nosrati R, Golichenari B, Rezaee R, Chatzidakis GI, Tsatsakis AM, Karimi G (2017) Nanomaterial-based aptasensors and bioaffinity sensors for quantitative detection of 17β-estradiol. TrAC Trends Anal Chem 94:95–105
4. Kuruca SE, Karadenizli S, Akgun-Dar K, Kapucu A, Kaptan Z, Uzum G (2017) The effects of 17β-estradiol on blood brain barrier integrity in the absence of the estrogen receptor alpha; an in-vitro model. Acta Histochem 119:638–647
5. Ganmaa D, Sato A (2005) The possible role of female sex hormones in milk from pregnant cows in the development of breast, ovarian and corpusuteri cancers. Med Hypotheses 65:1028–1037
6. López M, Tena-Sempere M (2017) Estradiol effects on hypothalamic AMPK and BAT thermogenesis: a gateway for obesity treatment? Pharmacol Ther 178:109–122
7. Chang HS, Choo KH, Lee B, Choi SJ (2009) The methods of identification, analysis, and removal of endocrine disrupting compounds (EDCs) in water. J Hazard Mater 172:1–12
8. Lu H, Xu S (2015) Mesoporous structured estrone imprinted Fe3O4@SiO2@mSiO2 for highly sensitive and selective detection of estrogens from water samples by HPLC. Talanta 144:303–311
9. Guenther K, Heinke V, Thiele B, Kleist E, Prast H, Raecker T (2002) Endocrine disrupting nonylphenols are ubiquitous in food. Environ Sci Technol 36:1676–1680
10. Janssens G, Mangelinckx S, Courtheyn D, De KN, Matthijs B, Le BB (2015) Simultaneous detection of androgen and estrogen abuse in breeding animals by gas chromatography-mass spectrometry/combustion/isotope ratio mass spectrometry (GC-MS/C/IRMS) evaluated against alternative methods. J Agric Food Chem 63:7574–7581
11. Zhang G, Li T, Zhang J, Chan A (2018) A simple FRET-based turn-on fluorescent aptasensor for 17β-estradiol determination in environmental water, urine and milk samples. Sensors Actuators B Chem 273:1648–1653
12. Silva CP, Lima DLD, Schneider RJ, Otero M, Esteves VI (2013) Evaluation of the anthropogenic input of caffeine in surface waters of the north and center of Portugal by ELISA. Sci Total Environ 124:227–232
13. Kanso H, Inguimbert N, Istamboulie G, Barthelmebs L, Calasblanchard C, Noguer T (2017) Chemiluminescence immunoassays for estradiol and ethinylestradiol based on new biotinylated estrogen derivatives. Anal Biochem 537:63–68
14. Akki SU, Werth CJ (2018) Critical review: DNA Aptasensors, are they ready for monitoring organic pollutants in natural and treated water sources? Environ Sci Technol 52:8989–9007
15. Fenzl C, Nayak P, Hirsch T, Wolfbeis SO, Alshareef NH, Baeumner JA (2017) Laser-scribed graphene electrodes for aptamer-based biosensing. ACS Sens 2:616–620
16. Svobodová M, Skouridou V, Botero ML, Jauset-Rubio M, Schubert T, Bashammakh AS, El-Shahawi MS, Alyoubi AO, O'Sullivan CK (2017) The characterization and validation of 17β-estradiol binding aptamers. J Steroid Biochem Mol Biol 167:14–22
17. Wang J, Coffey PD, Swann MJ, Yang F, Lu JR, Yang X (2010) Optical extinction combined with phase measurements for probing DNA-small-molecule interactions using an evanescent waveguide biosensor. Anal Chem 82:5455–5462
18. Kim YS, Jung HS, Matsuura T, Lee HY, Kawai T, Gu MB (2007) Electrochemical detection of 17beta-estradiol using DNA aptamer immobilized gold electrode chip. Biosens Bioelectron 22:2525–2531
19. Huang KJ, Liu YJ, Zhang JZ, Cao JT, Liu YM (2015) Aptamer/au nanoparticles/cobalt sulfide nanosheets biosensor for 17β-estradiol detection using a guanine-rich complementary DNA sequence for signal amplification. Biosens Bioelectron 67:184–191
20. Zhu B, Alsager AO, Kumar S, Hodgkiss JM, Travas-Sejdic J (2015) Label-free electrochemical aptasensor for femtomolar detection of 17β-estradiol. Biosens Bioelectron 70:398–403
21. Nie Y, Yuan X, Zhang P, Chai Y, Yuan R (2019) Versatile and ultrasensitive electrochemiluminescence biosensor for biomarker detection based on nonenzymatic amplification and aptamer-triggered emitter release. Anal Chem 91:3452–3458
22. Liu Y, Tuleouva N, Ramanculov E, Revzin A (2010) Aptamer-based electrochemical biosensor for interferon gamma detection. Anal Chem 82:8131–8136
23. Iranifam M (2013) Analytical applications of chemiluminescence-detection systems assisted by magnetic microparticles and nanoparticles. TrAC Trends Anal Chem 51:51–70
24. Yang R, Song D, Fang S, Liu Y, Zhou X, Long F, Zhu A (2018) Development of novel portable and reusable fiber optical chemiluminescent biosensor and its application for sensitive detection of microcystin-LR. Biosens Bioelectron 121:27–33
25. Song D, Yang R, Fang S, Liu Y, Long F (2018) A FRET-based dual-color evanescent wave aptasensor for simultaneous fluorometric determination of aflatoxin M1 and ochratoxin A. Microchim Acta 185:508–513
26. Chen A, Yan M, Yang S (2016) Split aptamers and their applications in sandwich aptasensors. Trends Anal Chem 80:581–593
27. Huang PJJ, Kempaiah R, Liu J (2011) Synergistic pH effect for reversible shuttling aptamer-based biosensors between graphene oxide and target molecules. J Mater Chem 21:8991–8993
28. Daniel C, Mélaïne F, Roupioz Y, Livache T, Buhot A (2013) Real time monitoring of thrombin interactions with its aptamers: insights into the sandwich complex formation. Biosens Bioelectron 40:186–192
29. Lautner G, Balogh Z, Gyurkovics A, Gyurcsányi RE, Mészáros T (2012) Homogeneous assay for evaluation of aptamer-protein interaction. Analyst 137:3929–3931
30. Liu J, Bai W, Niu S, Zhu C, Yang S, Chen A (2014) Highly sensitive colorimetric detection of 17β-estradiol using split DNA aptamers immobilized on unmodified gold nanoparticles. Sci Rep 4:7571